Available online at www.sciencedirect.com
SCIENCE DIRECT
Polymer 46 (2005) 9871–9880
polymer
www.elsevier.com/locate/polymer

Properties of poly(butylene terephthatlate) polymerized from cyclic oligomers and its composites

Hilde Parton[a,*], Joris Baets[a], Pascale Lipnik[c], Bart Goderis[b], Jacques Devaux[c], Ignaas Verpoest[a]

[a]Department of Metallurgy and Materials Science, K.U.Leuven, Kasteelpark Arenberg 44, B-3001 Leuven, Belgium
[b]Department of Chemistry, K.U.Leuven, Celestijnenlaan 200F, B-3001 Leuven, Belgium
[c]Unité de chimie et de physique des hauts polymères, U.C.L, Croix du Sud, 1, B-1348 Louvain-la-Neuve, Belgium

Received 29 November 2004; received in revised form 14 June 2005; accepted 27 July 2005
Available online 15 August 2005

Abstract

The high viscosity of thermoplastic matrices hampers fiber impregnation. This problem can be overcome by using low viscous polymeric precursors such as cyclic butylene terephthalate (CBT® resins), which polymerize to form a thermoplastic matrix. This allows thermoset production techniques, like resin transfer molding (RTM), to be used for the production of textile reinforced thermoplastics. Due to the processing route and more specifically the time–temperature profile, inherent to the RTM process, the crystallites of the matrix consist out of well-defined, thick and well-oriented crystal lamellae. Together with a high overall degree of crystallinity and a low density of tie molecules, these large and perfect crystals cause polymer brittleness. Matrix brittleness lowers the transverse strength of unidirectional composites to below the matrix strength, but leaves the mechanical properties in the fiber direction unaffected. Although not a valid option for the RTM production route, crystallization from a truly random melt and at a sufficiently high cooling rate would substantially improve the ductility.

Keywords: Crystallinity; Mechanical properties; Composites

1. Introduction

Interest in thermoplastic composites has increased steadily over the last years due to their advantages over thermoset composites. These advantages include improved toughness, impact resistance and added recycling options through reprocessing. The main drawback in using thermoplastic matrices is their high melt viscosity, which significantly hampers the impregnation of the fibrous reinforcement. Two main routes can be followed in order to facilitate impregnation, namely decreasing the matrix flow distance by, e.g. using commingled yarns, or decreasing the viscosity during impregnation [1]. If the viscosity of the thermoplastic matrix can be lowered sufficiently, production techniques typically associated with thermoset composites, such as resin transfer molding (RTM), can be used with minor adaptations to process thermoplastic composites.

Thermoplastic RTM, where polymeric precursors impregnate the continuous reinforcement after which a chemical reaction takes place to form the thermoplastic matrix, has recently received increasing attention [2–10]. Due to the constraints posed by both the in situ polymerization and the liquid molding process [11], only a limited amount of polymer systems are available for thermoplastic RTM, including the anionic ring-opening polymerization of polyamides and the entropically driven ring-opening polymerization of cyclic oligoesters. This paper focuses on the polymerization of cyclic(butylene terephthalate) oligomers (CBT® resin), to form the engineering thermoplastic poly(butylene terephthalate), (PBT).

The crystal structure of PBT crystallized from the melt and from dilute solution has been studied extensively. PBT has a triclinic unit cell for both known polymorphs, α being the predominant polymorph, whereas the β polymorph is only observed in drawn and spun fibers [12]. Besides the existence of two polymorphs, Stein and Misra observed two types of spherulitic superstructures depending on the crystallization temperature [13]. Controversy still exists

* Corresponding author. Tel.: +32 16 32 11 93; fax: +32 16 32 19 90.
E-mail address: hilde.parton@mtm.kuleuven.be (H. Parton).

0032-3861/$ - see front matter © 2005 Elsevier Ltd. All rights reserved.
doi:10.1016/j.polymer.2005.07.082

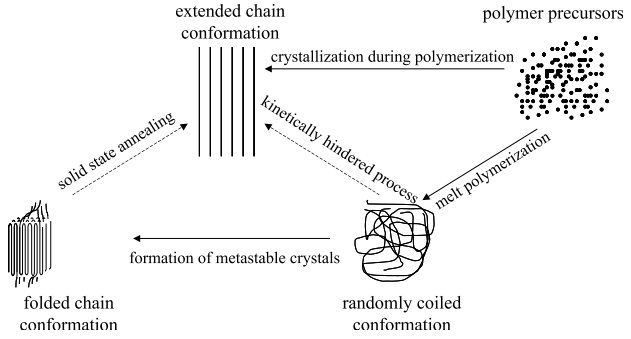

Fig. 1. Crystal conformation according to Wunderlich [19].

concerning the assignment of the multiple melting behavior of PBT to the existence of these two spherulitic superstructures [13–17] as well as on the effect of these superstructures on the mechanical properties. Möginger [18] observed an increase in amount of usual type spherulites when the cooling rate decreased and the melt temperature increased. Together with the increasing amount of usual type spherulites, PBT became more brittle, reducing the strain at failure from more than 30 to less than 4%. The increase in overall crystallinity was, however, not discussed. Ludwig and Eyerer [14] on the other hand observed an increase in yield stress for the usual type spherulites, but could not find a decrease in strain at the yield point. They also do not report on a difference in strain at failure.

The processing route followed in thermoplastic RTM differs from conventional processing of, e.g. compression molded PBT composites from commingled yarns, where PBT is crystallized from the melt. Since the melting point of the CBT® resin is below that of PBT and the conversion from CBT oligomers to PBT is sufficiently rapid at relatively low temperatures, isothermal processing below the melting point of PBT is possible. Depending on the degree of supercooling and the reaction speed, this isothermal processing may result in simultaneous polymerization and crystallization.

According to Wunderlich [19], simultaneous polymerization and crystallization can lead to a very different crystal morphology ranging from a fully extended chain conformation to a folded chain conformation, which is the typical conformation for crystallization from the melt, Fig. 1. The tie molecule density can also be influenced by simultaneous polymerization and crystallization. Miller [20] stated that if oligomers are added to polymer chains that already began to crystallize, only short amorphous segments are attached to crystal growth fronts, which in turn have a low probability of becoming part of more than one lamellae thus forming tie molecules.

In this study, the effect of the processing route used in thermoplastic RTM on the crystal structure and mechanical properties of polymerized CBT® resin and its composites is investigated.

2. Experimental

2.1. Materials

CBT® resin was supplied in powder form by Cyclics Corporation. The number of butyl groups in the oligomer mixture varies from two to seven, resulting in a melting range from 130 to 160 °C. Before processing, the oligomers were dried overnight at 110 °C to remove residual moisture, which could interfere with the polymerization reaction. The tin-based transesterification catalyst (Fascat™ 4101) is commercially available from Atofina Chemicals Incorporated. Polymerized CBT® resin will from hereon be referred to as pCBT.

The reinforcements used were two mainly unidirectional, non-crimp glass fiber fabrics, which were also dried overnight at 110 °C before processing. The first non-crimp fabric (S-UD) supplied by Saertex Wagener GmbH has a total areal density of 951 g/m^2. Although this fabric is mostly unidirectional, a small amount of 90° fibers (27 g/m^2) was added to ensure fabric stability. Three layers of this fabric were used, resulting in a total fiber volume fraction of 54% for a composite thickness of 2 mm.

Ahlstrom supplied the second type of non-crimp fabric (A-UD), which consists out of three plies, 0, 90° and a random mat. The areal density of these individual plies was determined experimentally resulting in, respectively, 1217, 60 and 53 g/m^2. Two fabrics were used $(0, R, 90)_s$ to reach a fiber volume fraction of 52% for a 2 mm thick composite.

Injection molded plates ($6\times6\times2$ mm^3) of commercially available PBT, namely Ultradur B4500, were supplied by BASF-AG. This material will be simply referred to as PBT. Glass fiber reinforced PBT composites were produced from the melt by compression molding PBT Twintex® supplied by Vetrotex Renforcement S.A.

2.2. Production process

The production of glass fiber reinforced polymerized CBT (GF-pCBT) closely resembles the well-known RTM process for thermoset composites. The oligomers are heated to a temperature (190 °C) above their melting point, after which the catalyst (0.45 wt%) is added. The resulting mixture is stirred for a well-defined time (15 s), before it is vacuum infused into the closed mold, containing the fibrous reinforcement. During this stirring time, polymerization already commences, resulting in a continuously increasing viscosity and thus a limited time window for impregnation. The effect of the (rather short) stirring time on the final properties was not investigated. Once the mold is completely filled, in- and outlet ports are closed after which sufficient time (30 min) should be available to complete the polymerization reaction and crystallization (at the polymerization temperature). Flat plates ($320\times200\times2$ mm^3) of both unreinforced pCBT and GF-pCBT were produced.

2.3. Reprocessing

A lab-scale injection molding machine was used to produce tensile bars, starting from both the unreinforced, grinded pCBT and PBT. The melt temperature was around 250 °C whereas the mold was kept at room temperature.

2.4. Molecular weight and degree of conversion

Gel permeation chromatography (GPC) was used to determine the molecular weight as well as the oligomer conversion. The measurements were performed with a mixture of chloroform/hexafluoro-2-propanol (HFIP) as solvent (98/2 $CHCl_3$/HFIP). The flow rate was 0.8 ml/min at a temperature of 20 °C. Two Waters PL HFIPgel columns were used in series. The chromatograph was connected to a Waters 484 UV detector working at 254 nm. In order to relate retention time to molecular weight, a universal calibration was made using various polystyrene standards. For sample preparation, approximately 2 mg of matrix was dissolved in 80 μl of HFIP. After total dissolution, the solution was diluted by 4 ml of chloroform.

The degree of conversion was determined from these GPC measurements by comparing the amount of remaining oligomers to the amount of polymer and is calculated according to Eq. (1)

$$\alpha = 1 - \frac{A_{\text{oli}}}{A_{\text{tot}}} \tag{1}$$

with A_{oli} the area under the oligomer peaks of the retention time curve and A_{tot} the total area under the retention time curve.

2.5. Differential scanning calorimetry (DSC)

A T.A. Instruments 2920 DSC was used to investigate the isothermal crystallization kinetics of catalyzed CBT as well as to determine the degree of crystallinity, defined in Eq. (2), in the produced samples.

$$\chi_{\text{c,DSC}} = \frac{\Delta H_{\text{m}}}{\Delta H_{\infty}} \tag{2}$$

where ΔH_{m} is the melting enthalpy of the polymer, and ΔH_{∞} is the melting enthalpy of the fully perfect crystal of PBT, which is found in literature to be 142 J/g [21]. Melting endotherms were recorded at 10 °C/min and the melting enthalpy of the polymer was determined by integrating the area under the normalized melting peak after subtraction of an arbitrary baseline.

2.6. Wide angle X-ray diffraction (WAXD)

Scattering patterns of the unreinforced pCBT were obtained in transmission mode with a Rigaku Rotaflex RTP 30RC goniometer. The experiments used Cu K_α radiation (40 kV–100 mA) and the angular range covers $5° < 2\theta < 60°$, with 2θ the scattering angle. The resulting patterns were corrected by subtracting both a scaled empty cell measurement and a linear background. The shape of the amorphous halo was determined by quenching CBT® resin and recording the scattering pattern. This halo was then scaled to fit underneath the scattering pattern of the samples to determine the integrated intensity of the amorphous halo (I_{a}). The degree of crystallinity was calculated according to Eq. (3), comparing the integrated intensity of the amorphous halo to the overall integrated intensity ($I_{\text{a}} + I_{\text{c}}$).

$$\chi_{\text{c,WAXD}} = 1 - \frac{I_{\text{a}}}{I_{\text{a}} + I_{\text{c}}} \tag{3}$$

Scattering patterns of fiber reinforced pCBT were obtained in reflection mode with a Siemens D500 goniometer. All experiments used Cu K_α radiation (40 kV–40 mA) and the angular range is $5° < 2\theta < 50°$.

2.7. Transmission electron microscopy (TEM)

The lamellar structure was investigated with TEM. First, the sample surfaces were prepared for contrast coloring. Then the samples were stained with ruthenium tetroxide by exposing them for 48 h to a $RuCl_3 \times NaClO$ vapor after which they were cut for the first time with a diamond knife. The staining procedure was repeated before recutting the samples and depositing them on a TEM grid. TEM micrographs were obtained on a LEO 922 transmission electron microscope operating at 200 kV. The samples obtained for TEM were also examined by polarized optical microscopy.

2.8. Small angle laser light scattering (SALLS)

SALLS was measured on an home-made vertical apparatus consisting of a polarized 1 mW Spectra-Physics 117A type He/Ne laser ($\lambda = 632.8$ nm), a polarizer set parallel to the polarization of the laser, the sample in a Mettler FP-82HT hot stage, a second polarizer (analyzer) oriented with its polarization perpendicular (Hv SALLS) to that of the first one, a screen with a beam catcher on which the scattering patterns are projected and a Photometrix ATC200L cooled CCD detector. The scattering angle is calibrated with a 100 lines/mm grid. Samples with a thickness of only a few times the spherulitic radius are needed for these tests. Therefore, for the CBT® resin, the specimens were molten in between two glass plates and subsequently polymerized and crystallized at 190 °C in a Mettler hot stage. The PBT samples were first molten in between the glass plates after which they were squeezed in order to obtain a thin film. These samples were subsequently placed into a Mettler hot stage at 250 °C after which they were quenched in air.

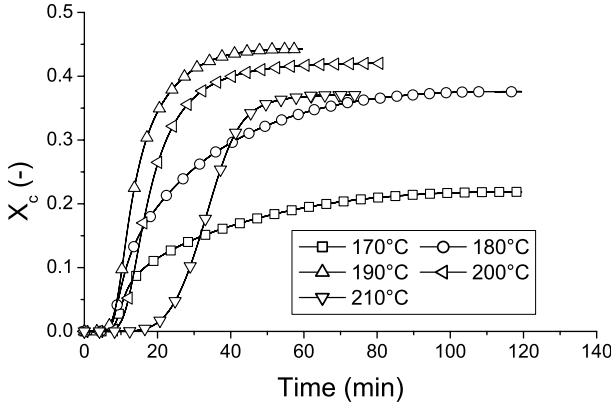

Fig. 2. Crystallization kinetics of catalyzed CBT® resin.

2.9. Mechanical properties

Both unreinforced pCBT and PBT and reinforced pCBT are tested in three point bending according to ASTM D790-84. In order to compare the moduli of the composites to their theoretical values, the longitudinal ply properties were calculated with the simple rule of mixtures whereas the transverse ply properties were calculated with the equation of Chamis [22]. Using these ply properties, the composite properties were calculated according to the classical laminate theory using the software Composite Star™.

Small unreinforced injection molded tensile bars were used for tensile testing of the reprocessed pCBT (RP-pCBT) and PBT (RP-PBT).

3. Results and discussion

3.1. Crystallization kinetics

Fig. 2 shows the degree of crystallinity as function of time for catalyzed CBT oligomers. Before crystallization can commence, these oligomers need to convert to polymer of sufficiently high molecular weight. Due to the athermal nature of this polymerization reaction, the exothermic peak during the DSC scan can be solely attributed to the crystallization [20].

Crystallization curves of melt crystallized PBT usually show a decrease in crystallinity and an increase in crystallization speed when the degree of supercooling increases [23,24]. If polymerization and crystallization were consecutive, meaning that molecular weight build-up was completed before the start of crystallization, the crystallization kinetics would not differ from melt-crystallized PBT, except for a time-shift equal to the time needed for polymerization. Since the crystallization curves presented here clearly differ from melt crystallized PBT, it can be concluded that for temperatures below 200 °C, where polymerization is relatively slow, polymerization and crystallization are simultaneous. As mentioned before, this simultaneity can affect the crystal structure, the final degree of crystallinity and hence the mechanical properties.

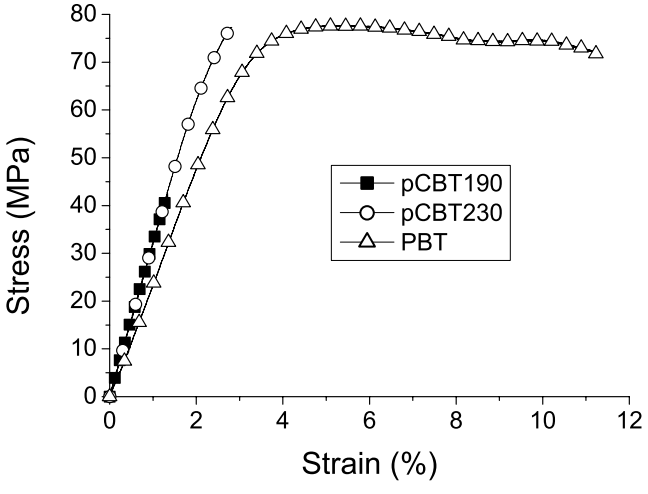

Fig. 3. Typical 3 point bending stress–strain curves for pCBT and PBT.

Table 1
Flexural properties of pCBT compared to PBT

	E (GPa)	σ^* (MPa)[a]	ε^* (%)[a]
pCBT, 190 °C	3.2±0.1	54±5	1.6±0.2
pCBT, 230 °C	3.1±0.2	73±14	2.3±0.7
PBT	2.2±0.1	73±11	3.3±0.3

[a] Stress and strain at break for pCBT, stress and strain at yield for PBT.

3.2. Mechanical properties

In order to assess the mechanical properties of pCBT, flexural tests were performed on pCBT, isothermally processed at 190 °C, pCBT polymerized at 230 °C and crystallized at 190 °C and classically produced PBT (rapid cooling from the melt). Typical stress–strain curves are depicted in Fig. 3 whereas the flexural properties are shown in Table 1. It is clear that the pCBT behaves differently from PBT. Apart from the higher modulus, pCBT breaks in a brittle manner whereas the PBT samples do not break at all in this three point bending test, but show a yield point.

The difference between simultaneous (at 190 °C) and consecutive (at 230 °C) polymerization and crystallization is smaller but still obvious. Although both samples are brittle, breaking at small strain levels, the samples prepared by consecutive polymerization and crystallization at 230 °C do exhibit higher strain to failure and higher strength.

There are a number of reasons why a thermoplastic polymer can be brittle. Apart from defects and impurities, a low molecular weight, a high degree of crystallinity, very large spherulites or a low density of (intercrystalline) tie molecules can substantially reduce ductility. Therefore, the specimens were characterized with special emphasis on the crystalline structure.

Table 2
Properties of pCBT compared to PBT

	M_n (kg/mol)	M_w (kg/mol)	α (%)	$\chi_{c,DSC}$ (%)	$\chi_{c,WAXD}$ (%)
pCBT, 190 °C	29.3±0.2	61.4±0.5	98.2±0.1	47±2	52
pCBT, 230 °C	35.0±0.4	73.3±0.6	98.7±0.1	42±2	49
PBT	33.8±0.4	69.3±0.2	98.8±0.1	35±1	31

Table 3
Crystallite size

	D_{001} (Å)	$D_{0\bar{1}1}$ (Å)	D_{010} (Å)
pCBT, 190 °C	103	134	241
pCBT, 230 °C	110	138	239
PBT	72	108	129

3.3. Physical properties

One of the first prerequisites to get a tough material is a high oligomer conversion and sufficient molecular weight build-up. The results shown in Table 2 show that the remaining oligomer content in the pCBT samples is equivalent to the equilibrium oligomer content in PBT, which is known to be 1–3% [25]. There are, however, slight differences in molecular weight, nevertheless the attained molecular weight exceeds the critical molecular weight for entanglements, $M_{w,c}$ of 50 kg/mol [20].

Fig. 4 shows a typical pCBT scattering pattern, with the fitted amorphous halo. As expected, the scattering pattern corresponds to the α polymorph. The degree of crystallinity determined from these diagrams as well as from the melting endotherms is also listed in Table 2. Despite the discrepancy between the two measurement techniques, both show a significantly higher degree of crystallinity for pCBT compared to PBT. This large difference in crystallinity is believed to be responsible for the elevated modulus of pCBT as compared to PBT.

Fig. 5 compares the scattering patterns of pCBT and PBT clearly showing not only the difference in degree of crystallinity but also in crystallite size and perfection. Large and perfect crystals give rise to narrow peaks as seen for pCBT. The difference in crystallite size can be quantified by using the Scherrer equation, Eq. (4), which relates the peak width to the crystallite size

$$D_{hkl} = \frac{\lambda}{\beta_{hkl}\cos\theta_{hkl}} \tag{4}$$

where λ is the wavelength, θ half the Bragg angle and β_{hkl} the integral breadth of the *hkl* diffraction peak. For some well-defined peaks, the results are shown in Table 3.

Although expected, there is not a large difference in crystal structure between simultaneous and consecutive polymerization and crystallization, shown by the results presented above. Due to the constraints of the equipment used in thermoplastic RTM, cooling rates were small and hence crystallization was slow allowing for high degree of crystallinity and crystal perfection.

Fig. 6 shows the TEM micrographs of both PBT and pCBT. In contrast to the PBT sample, the lamellae in the pCBT samples are well defined, thicker and nicely oriented. Moreover, the transition from crystalline to amorphous is more pronounced and sharp in the pCBT samples, which might be an indication of a reduction of tie molecules.

As stated by Miller [20], the tie molecule density is influenced by simultaneous polymerization and crystallization. In the case of pCBT, the transesterification catalyst remaining in the polymer might also influence the amount of tie molecules. Indeed, the catalyst molecules cannot be included into the polymer crystal, but probably concentrate at the surface of the growing crystals. Owing to the mechanical tensions arising from packing density

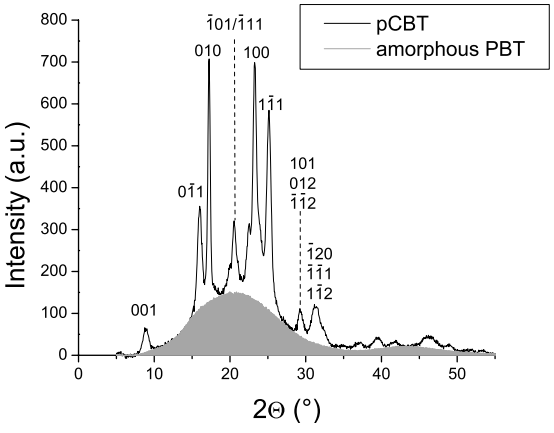

Fig. 4. pCBT Scattering pattern, showing amorphous halo and principal crystalline reflections.

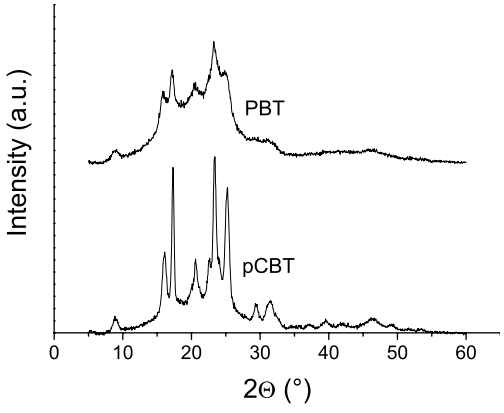

Fig. 5. WAXD pattern of pCBT and PBT.

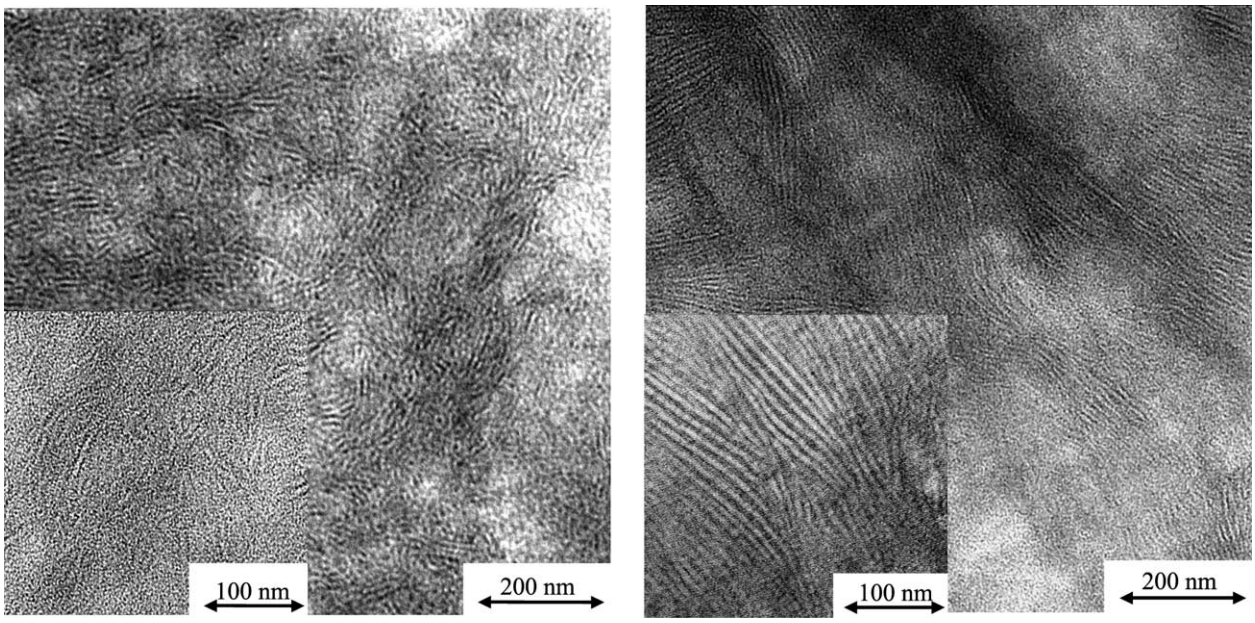

Fig. 6. TEM micrographs (left) PBT (right) pCBT.

differences at the crystal boundaries, such a local transesterification enhancement would drastically decrease the amount of tie molecules.

The optical micrographs shown in Fig. 7, depict a clear unusual spherulitic superstructure for the PBT samples, which is typically formed in fast crystallizing PBT [18]. The

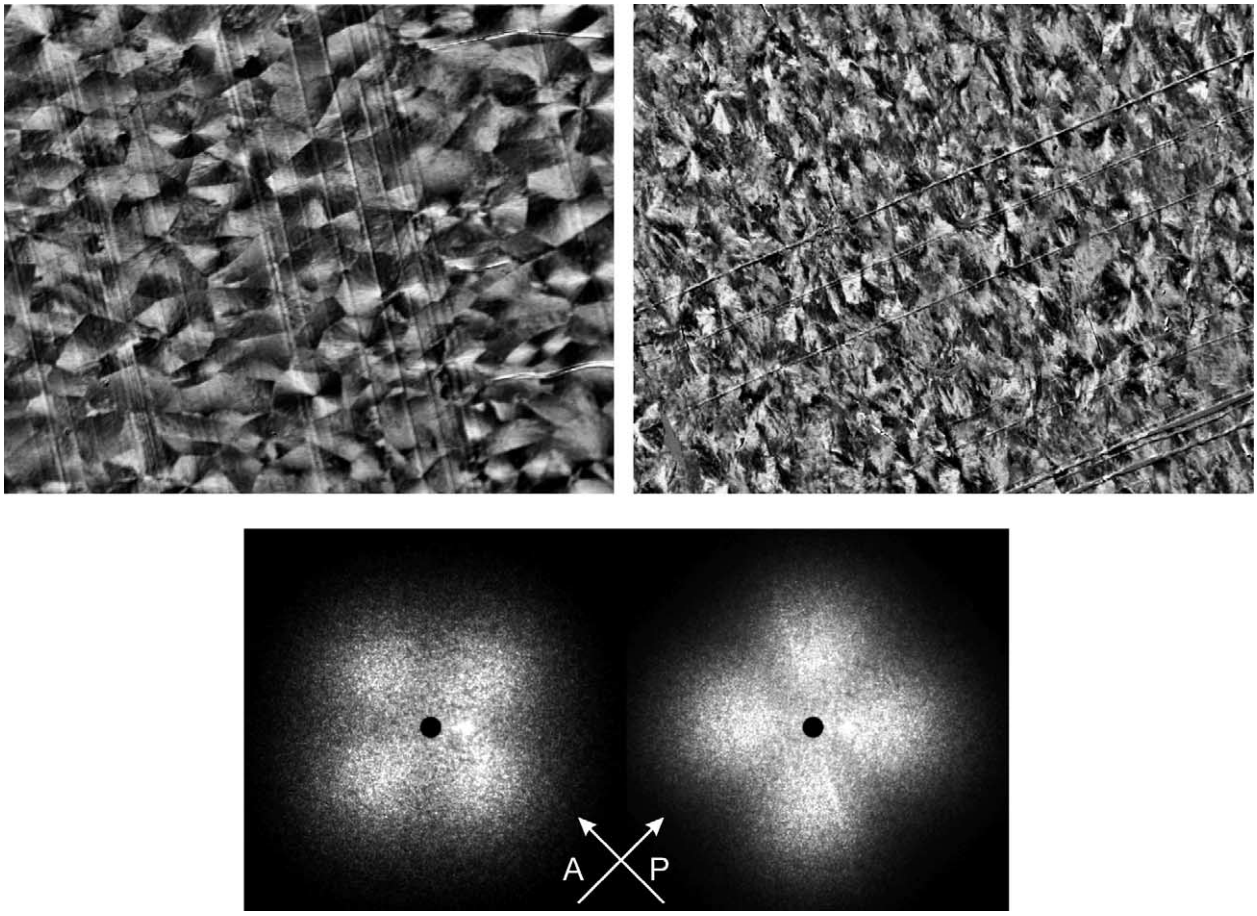

Fig. 7. Optical micrographs and corresponding light scattering patterns of PBT (left) and pCBT (right).

Fig. 8. Tensile samples after testing (left) RP-PBT (right) RP-pCBT.

pCBT samples on the other hand do not clearly show a spherulitic superstructure but show a superstructure that might indicate the ordering of lamellae in parallel stacks [26]. The corresponding small angle light scattering patterns, on the other hand, confirm the unusual spherulitic superstructure of PBT but also reveal a clear spherulitic superstructure for pCBT. This superstructure, however, consists of usual type spherulites, which is consistent with the observations of Stein and Misra [13].

3.4. Reprocessing of pCBT and PBT

From the results presented above, it is clear that pCBT is brittle when processed under similar conditions as it would be in RTM. In order to investigate the intrinsic ability of

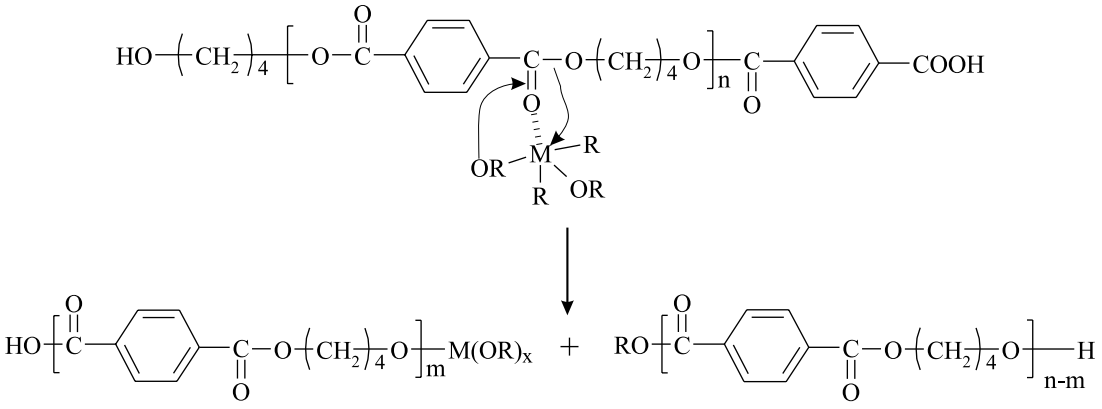

Fig. 9. Proposed mechanism for the molecular weight reduction in the presence of the catalyst [29].

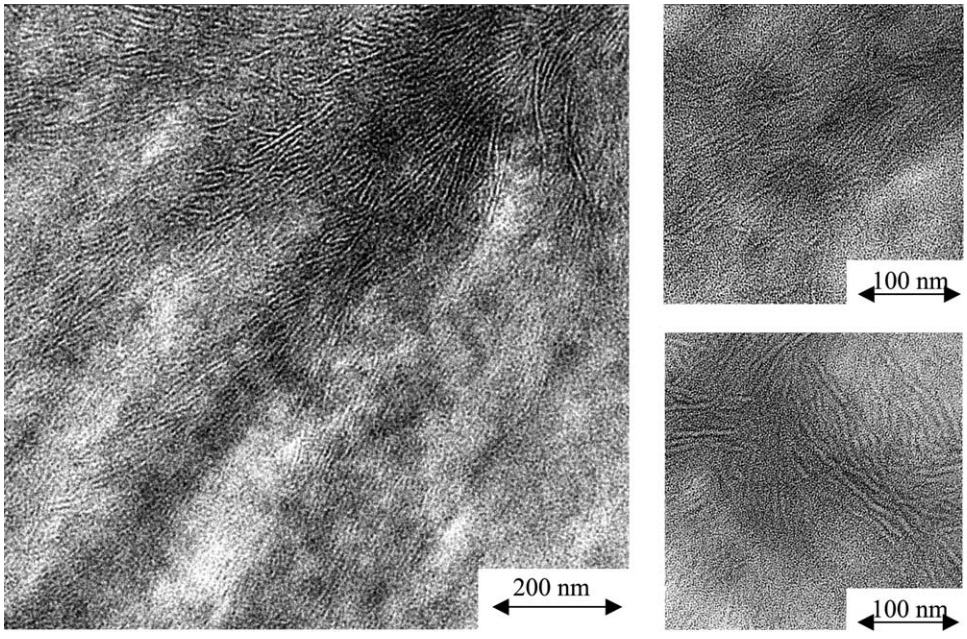

Fig. 10. TEM micrograph of RP-pCBT.

Table 4
Properties of RP-pCBT, RP-PBT compared to injection-molded pCBT

	E (MPa)	σ^* (MPa)	ε^* (%)	M_n (kg/mol)	M_w (kg/mol)	α (%)	χ_c (%)
RP-pCBT	2.3±0.2	46±7	3–70	20.5±1.9	40.6±4.3	97.9±0.1	35±2
RP-PBT	2.5±0.2	50±1	16–225	32.3±0.2	66.3±0.5	98.7±0.1	34±1
IM-pCBT	2.4	55	160	–	113	–	–

Table 5
Flexural properties of GF-pCBT

	E_{11} (GPa) [calc.]	E_{22} (GPa) [calc.]	σ_{11} (MPa)	σ_{22} (MPa)
S-UD	38.3±1.2 [39.4]	8.7±0.9 [10.0]	766±113	66±6
A-UD	37.8±1.4 [38.8]	6.8±1.8 [8.0]	901±64	96±4

pCBT to behave like a ductile material, both pCBT and PBT were grinded and reprocessed by injection molding (giving RP-PBT and RP-pCBT). The resulting tensile bars were tested and the broken specimens are shown in Fig. 8. Even though it is obvious that the RP-PBT shows more necking than the RP-pCBT, some of the latter samples clearly show neck formation and thus ductile behavior.

Table 4 shows the properties of the reprocessed specimens as well as some properties of injection molded CBT® resin (IM-pCBT), polymerized during molding and with a lower catalyst level (0.33 versus 0.45 wt%), [27,28]. The modulus of RP-pCBT decreased in comparison with pCBT but is now quite similar to both PBT and RP-PBT as is the yield strength.

The GPC-measurements revealed a large drop in molecular weight for the RP-pCBT compared to the pCBT, which is not as pronounced in RP-PBT. Hydrolysis of PBT in the presence of water is known to decrease the molecular weight and although the samples were dried before reprocessing, the commercial sample might contain stabilizers, which reduce the molecular weight reduction in the presence of water. Moreover, the rather high level of catalyst still present in the pCBT samples might have a negative effect on the molecular weight by a transesterification reaction that is shown in Fig. 9.

The resulting molecular weight of the RP-pCBT is lower than the critical molecular weight for molecular entanglement mentioned above. This limit was, however, deduced from previous tests of PBT with varying molecular weights [20] and must, therefore, not be seen as absolute. It is nevertheless clear that the molecular weight of the RP-pCBT is close to the critical molecular weight, therefore, not all specimens show necking. When the molecular weight of pCBT after injection molding is large enough, ductile behavior comparable to that of PBT is observed, Table 4.

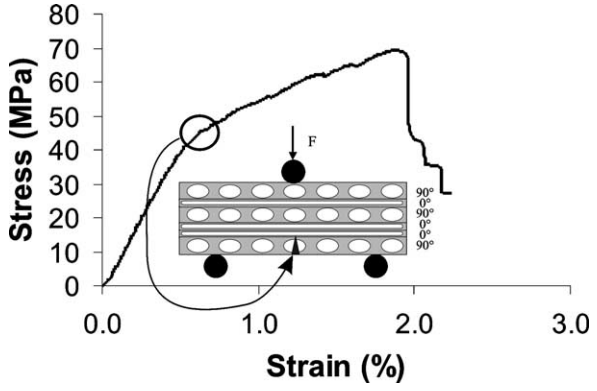

Fig. 11. Stress–strain curve of transverse flexural test of S-UD reinforced pCBT.

The WAXD pattern of the RP-pCBT resembles the original pattern of PBT. The TEM micrographs on the other hand revealed a non-homogeneous structure, Fig. 10. Although a structure very similar to PBT is present, some parts clearly exhibit better-defined, oriented and wider lamellae.

Even though the pCBT was grinded and molten before injection molding, some of its original structure was restored upon recrystallization, indicating lack of molecular entanglement probably due to insufficient homogenization at molecular level. The stagnant conditions during the polymerization of CBT above the melting point of PBT in the RTM-like process, can also lead to a lack of molecular entanglement. Together with the slow cooling rate, this might help to understand why the degree of perfection is similar to that of simultaneously polymerized and crystallized pCBT.

3.5. Properties of composites

Table 5 shows the flexural properties of the glass fiber reinforced pCBT. The calculated theoretical moduli compare well to the experimental values, both in longitudinal and transverse direction.

Fig. 11 shows the stress–strain behavior of the S-UD reinforced pCBT. Due to the nature of the fabric, containing not only 0° but also a small amount of 90° oriented fibers, this measured strength is actually an overestimation of the real transverse strength. The knee in this curve indicates failure of the outer layer, which does not induce total failure due to the 'cross-ply' nature of the specimen. Compared to the flexural strength of PBT, which is known to be in the range of 80–115 MPa [30], the real transverse strength is, however, quite low.

The transverse strength is a non-fiber dominated property and hence influenced by both the matrix and interface properties. In glass fiber composites, large local stress concentrations around the fibers exist because of the large stiffness mismatch between glass fibers and the polymer matrix. This initiates cracks normal to the loading direction either at the matrix–fiber interface or in the matrix [22]. These stress concentrations are responsible for lowering the transverse strength of thermoset composites below the strength of the matrix. Thermoplastic or toughened thermoset matrices on the other hand should be able to compensate for these stress concentrations by local plastic deformation of the matrix thus increasing the transverse strength to above the matrix strength [31,32].

A low transverse strength is, therefore, an indication of either poor fiber–matrix interface properties or matrix brittleness. Glass fiber reinforced pCBT prepared with commercially available 'epoxy-compatible' sized fibers

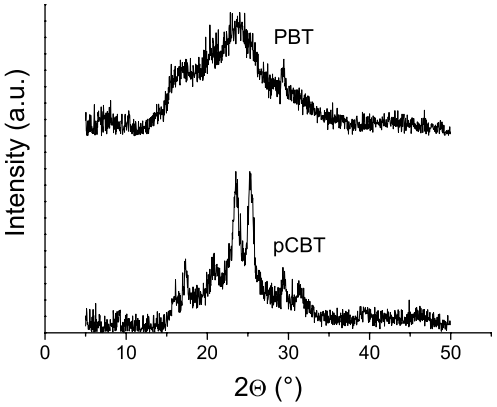

Fig. 12. Diffraction pattern of glass fiber reinforced PBT (Twintex®) and pCBT.

should have adequate interface properties. Bahr [27] showed that compared to pCBT composites made from unsized glass fibers, the interlaminar shear strength improved substantially (63 versus 24 MPa). Compared to glass fiber reinforced epoxy on the other hand, this ILSS was somewhat lower but the pCBT samples did show some yielding. Based on the results for unreinforced pCBT, it is, however, very likely that the low transverse strength is caused by matrix brittleness.

In order to assess the crystal structure of the matrix when fibers are present, WAXD diffraction patterns were recorded for both glass fiber reinforced PBT (Twintex®) and pCBT, Fig. 12. Although it is not possible to distinguish between the polymer amorphous halo and the halo originating from the glass fibers and hence determining the degree of crystallinity, the difference in crystal perfection is again obvious. The presence of the glass fibers does not interfere with the formation of large and perfect crystals.

4. Conclusions

Infusing low viscous thermoplastic prepolymers into a fiber preform to produce textile reinforced thermoplastics seems to be very promising since it combines both the advantages of thermoplastics and the ease of impregnation of thermoset resins. Due to the difference in processing route, matrix properties differ from classically produced composites.

The production route of CBT® resins in an RTM like process gives rise to well-defined, thick and well-oriented lamellae and a high overall degree of crystallinity. Together with a low density of tie molecules, these large and perfect crystals cause polymer brittleness. When polymerization and crystallization were consecutive under stagnant conditions and the cooling rate was low, similar crystal perfection was obtained. Reprocessing of the brittle polymer partially destroys the crystal structure resulting in a more ductile material. If CBT® resins are crystallized from a truly random melt at a sufficiently high cooling rate, they will behave as classical injection molded PBT.

Non-isothermal processing, that is rapidly cooling down the matrix from the melt is not an option in thermoplastic RTM since it would drastically increase cycle times. Other solutions, therefore, need to be explored in order to allow for a reduction in degree of crystallinity and maybe more important in crystal perfection.

The mechanical properties of the resulting composites are not at all affected in fiber dominated orientations. The transverse strength on the other hand decreased to below the matrix strength due to the brittleness of the matrix.

Acknowledgements

The authors wish to thank the FWO-Vlaanderen for funding the PhD-grant of H. Parton and the postdoctoral fellowship of B. Goderis. Cyclics Corporation, BASF and Vetrotex Renforcement are acknowledged for supplying materials.

References

[1] Miller A, Gibson AG. Polym Polym Compos 1996;4(7):459.
[2] Greaney M, Ó Bradaigh CM. Proceedings of Sampe Europe Conference, Paris, 2003. p. 677.
[3] Gittel D, Callies H, Eyerer P, Ludwig HC, Möginger B. Proceedings of ICCE/6, Florida, 1999. p. 251.
[4] Luisier A, Bourban PE, Manson JAE. J Appl Polym Sci 2001;81(4):963.
[5] Luisier A, Bourban PE, Manson JAE. Composites Part A 2003;34:583.
[6] Mairtin PO, McDonnell P, Connor MT, Eder R, Ó Bradaigh CM. Composites Part A 2001;32(7):915.
[7] Pillay S, Ning H, Vaidya UK, Janowski GM. Proceedings of FPCM7 Newark, Delaware, USA, 2004. p. 65.
[8] van Rijswijk K, Vlasveld DPN, Bersee HEN, Picken SJN. Proceedings of ICCST-4, Durban, South Africa 2003.
[9] Verrey J, Michaud V, Manson JAE. Proceedings of 24th international Sampe Europe conference, Paris, 2003. p. 553.
[10] Parton H, Verpoest I. Proceedings of 7FPCM-7 Newark, Delaware, USA, 2004. p. 57.
[11] Parton H, Verpoest I. Polymer Composites 2005;26(1):60.
[12] Carr PL, Jakeways R, Ward IM. J Polym Sci, Part B: Polym Phys 1997;35:2465.
[13] Stein RS, Misra A. J Polym Sci, Polym Phys Ed 1980;18:327.
[14] Ludwig HJ, Eyerer P. Polym Eng Sci 1988;28(3):143.
[15] Al-Raheil IS, Qudah AMA. Polym Int 1995;37:47.
[16] Yasuniwa M, Tsubakihara S, Ohoshita K, Tokudome S. J Polym Sci, Part B: Polym Phys 2001;39:2005.
[17] Yeh JT, Runt J. J Polym Sci, Part B: Polym Phys 1989;27:1543.
[18] Möginger B, Lutz C, Polsak A, Fritz U. Kunststoffe 1991;81(3):251.
[19] Wunderlich B. Adv Polym Sci 1968;5:568.
[20] Miller S. Macrocyclic polymers from cyclic oligomers of poly-(butylene terephthalate). PhD dissertation. Amherst: University of Massachusetts; 1998.
[21] Vendramini J, Bas C, Merle G, Boissonnat P, Alberola ND. Polym Compos 2000;21(5):724.

[22] Mallick PK. Fiber-reinforced composites. 2nd ed. New York: Marcel Decker; 1993.
[23] Kulshreshtha B, Ghosh AK, Misra A. Polymer 2003;44:4723.
[24] Park CS, Lee KJ, Kim SW, Lee KY, Nam JD. J Appl Polym Sci 2002; 86:478.
[25] Brunelle DJ, Bradt JE, Serth-Guzzo J, Takekoshi T, Evans TL, Pearce EJ, et al. Macromolecules 1998;31(15):4782.
[26] Peeters M, Goderis B, Vonk C, Reynaers H, Mathot V. J Polym Sci, Part B: Polym Phys 1997;35:2689.
[27] Bahr SR. Proceedings of functional fillers for plastics, Atlanta 2003.
[28] Bahr SR. Personnal communication; 2004.
[29] Brunelle DJ. Cyclic oligomers of polycarbonates and polyesters. In: Smeylen JA, editor. Cyclic polymers. Dordrecht: Kluwer Academic Publishers; 2000. p. 185.
[30] Muzzy JD. Thermoplastics-properties. In: Kelly A, Zweben C, editors. Comprehensive composite materials. Amsterdam: Elsevier Science; 2000. p. 57.
[31] d'Hooghe EL, Hoek B, Edwards CM. Proceedingd of EPTA 5th world pultrusion conference, Leusden, The Netherlands 2000.
[32] Sumerak JE. Proceedings of EPTA 7th world pultrusion conference, Amsterdam 2004.